

Refined plastic hinge analysis of steel frames under fire

S.L. Chan[†] and B.H.M. Chan[‡]

*Department of Civil and Structural Engineering, The Hong Kong Polytechnic University,
Hong Kong SAR, Hong Kong*

Abstract. This paper presents an effective, reliable and accurate method for prediction of structural behaviour of steel frames at elevated temperature. The refined plastic hinge method, which has been used successfully in the second-order elasto-plastic analysis of steel frames at ambient conditions, is adopted here to allow for time-independent fire effects. In contrast to the existing rigorous finite element programs, the present method uses the advanced analysis technique that provides a simple and reliable means for practical study of the behaviour of steel frames at elevated temperature by a limiting stress model. The present method is validated against other test and numerical results.

Key words: elastic-plastic analysis; plastic hinge analysis; steel frames; elevated temperature; fire.

1. Introduction

Traditionally, structural engineers provide nominal fire protections to structural elements at a prescriptive fire rating. However, the method may not be effective in real fire cases and the cost of conventional fire protections can be as high as 30% of the total cost of steelwork (Lawson 1987). With the emergence of recent performance-based design regulations in various countries, it is necessary for structural engineers to grasp a thorough understanding of behaviour of structures under fire and to adopt the more reliable and cost effective performance-based design procedure.

A worthwhile application of fire engineering structural design will be the study of stability, strength and deformation characteristics of structures under factored loads but at an elevated temperature. The effect of thermal expansion for moderate change in temperature can be allowed in a simple manner in a frame analysis software. However, the drastic change of material properties under fire requires a considerable modification in the analysis procedure.

Owing to the limited size of tested specimen and experimental cost, extensive work was conducted on numerical simulation of steel frames under fire. Furumura and Shinohara (1978) adopted a bi-linear simplified model for stress vs. strain relation of steel material under elevated temperature. The effect of creep and thermal expansion were considered and it represented an early work utilising the Newton-Raphson procedure for large deflection analysis of steel frames. Saab and Nethercot (1991) proposed a numerical procedure for two dimensional analysis of steel frames by increasing the temperature and keeping the external load constant. The effect of creep was ignored explicitly since the heat-rate is not sensitive for temperature rate of 10-50°C/minute. Poh and Bennetts (1995) analysed steel columns under fire and compared their results against

[†]Professor

[‡]Ph.D. Candidate

experimental measurement. Wang and Moore (1995) used the finite element method for large deflection and material non-linear analysis of steel frames under fire. Both two and three dimensional cases were considered but only validation against two dimensional frames was conducted because of the lack of experimental data for three dimensional frames. Bailey (1998) used a sophisticated frame analysis program for 3-dimensional analysis of steel frames. Warping degree of freedom is considered, but no detail was given on warping transfer across connections. Even for static analysis under ambient temperature, the mechanism of warping transfer was not well researched and nearly all tested semi-rigid connections ignore this warping transformation. Song *et al.* (2000) used the effective integrated adaptive scheme for analysis of steel frames under fire and explosion. Liew *et al.* (1988) extended their "advanced analysis" to allow for fire.

In daily practical design, the solution is sought on the load capacity of structures under a certain time period of exposure to fire, which can be related to the temperature rise by various codes or recommendations. Most of the current literatures are based on a procedure of incrementing the temperature whilst keeping the load constant. This represents a typical response and load sequence. However, the simple procedure does not guarantee numerical convergence since the structure may not be able to retain the load at the specific temperature which is unknown in advance. If deflection criterion etc. is not used, numerical divergence is normally considered to be coincident with the structure failure, which is obviously unreliable since size of temperature increment may affect convergence. In some situations, an imposed live load may be applied or relieved to the heated members or frames due to passage of escapers during fire, the falling off of other structural and non-structural elements or burning off of some loads. Consequently, a software for this type of non-linear analysis under fire should possess two options of incrementing either the load or the temperature. Nevertheless, this consideration is only essential for path-dependent analysis involving strain reversal and unloading. For path-independent analysis using the dictated stress strain curve in various design codes, the results for these two analyses are invariant and both methods can then be used. The consideration of selecting either one of them is solely dependent on the numerical performance and convenience. It must further be emphasised that the numerical scheme is not linked with the isothermal or anisothermal assumptions for specimen testing and the present method can use the test results from either one of these testing procedures. Another advantage for using the present load incrementation scheme is on the consistency and physically rational failure criterion of using the limit load as the load capacity under a certain temperature. The controversial deflection failure criterion of one-twentieth of structural span or 1.5% strain etc. can be skipped in the present approach.

This paper is addressed to the development and implementation of a numerical scheme for efficient and effective large deflection analysis of steel frames using the bi-linear stress strain curve under elevated temperature. This concept follows the semi-rigid design in Eurocode 3 (1993) of replacing an arbitrary moment versus rotation curve by a bi-linear model. The present work is to satisfy the need of performance-based design in practice. The technique is in fact an extension of the refined plastic hinge method by the section assemblage concept (Chan and Chui 1997) which has been used with success in the analysis and performance-based design of steel structures. The concept assumes flanges take moment and web takes axial force and shear in construction of the yield and plastic surfaces. Using the Updated Lagrangian framework, the method can account for both the geometrical and material non-linear effects, including initial geometrical imperfections, semi-rigid connections and residual stresses under various temperature-dependent stress-strain relationships. Owing to the lack of experimental data in three dimensional frames, only planar steel frames made up of I-sections are considered in this paper. The results obtained from the proposed method are compared with

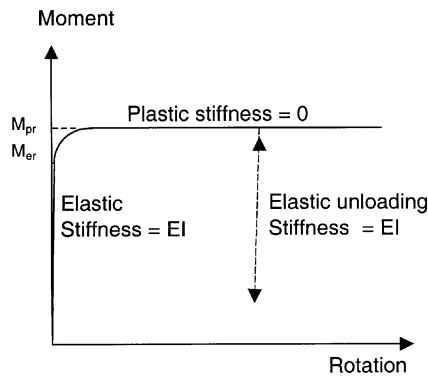


Fig. 1 Typical moment-rotation relationship of steel cross-sections

those by other investigations. Using this incrementation scheme and the section assemblage concept, the proposed procedure is more simple, reliable and stable than other numerical methods.

2. Basic assumptions

The following assumptions have been employed for the formulation.

- 1) Moment versus rotation is assumed as elasto-plastic while the first yield and fully plastic moments are constructed by a bi-linear stress-strain model using 0.2% proof stress. The moment-rotation relationship of cross-sections shown in Fig. 1 is assumed.
- 2) The analysis is path-independent and the loads are conservative.
- 3) The time-independent approach for structural fire analysis is adopted and the structural behaviour is therefore independent of the heating history.
- 4) Uniform heating along steel members and across cross sections is assumed.
- 5) Plasticity is considered at element ends only and governed by direct stresses due to bending moment and axial force.
- 6) Bernoulli hypothesis is assumed, i.e., a plane cross-section remains plane during deformation. Warping and shear deformation are not considered.
- 7) Steel members and frames are adequately restrained from out-of-plane deflection.

3. Mechanical constitutive relationships at elevated temperature

At elevated temperature, the sectional strength and stiffness of steel members reduces because of degradation of its mechanical properties and the influence of creep. Recently, it was also concluded by Talamona *et al.* (1997) that the most important factor to affect behaviour of steel columns is the effective values of yield stress at elevated temperature. In the present study, the Ramberg-Osgood equation (1943) used for approximation of the British test data (Kirby and Preston 1988) is adopted and expressed as,

$$\varepsilon_{\theta} = \frac{\sigma_{\theta}}{E_{20}} + \frac{3}{7} \frac{\sigma_{y20}}{E_{20}} \left(\frac{\sigma_{\theta}}{\sigma_{y20}} \right)^{50} \quad \text{for } 20^{\circ}\text{C} \leq \theta \leq 80^{\circ}\text{C} \quad (1)$$

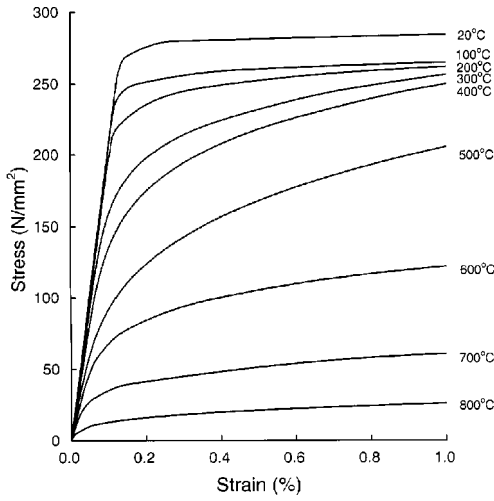


Fig. 2 Time-dependent stress-strain relationships based on the Ramberg-Osgood approximation

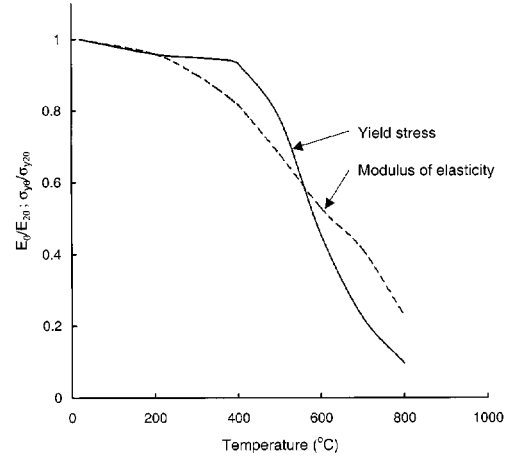


Fig. 3 Variations of yield stress and modulus of elasticity at elevated temperature

$$\varepsilon_{\theta} = \frac{\sigma_{\theta}}{E_{\theta}} + 0.01 \left(\frac{\sigma_{\theta}}{\sigma_{y\theta}} \right)^{\zeta_{\theta}} \quad \text{for } 80^{\circ}\text{C} < \theta \leq 800^{\circ}\text{C} \quad (2)$$

in which ε_{θ} and σ_{θ} are respectively the strain and the stress at a particular temperature, θ ; σ_{y20} and E_{20} are the yield stress and the modulus of elasticity of steel at room temperature of 20°C ; and $\sigma_{y\theta}$ is the effective yield stress, which is taken as the 0.2% proof stress at temperature, θ . These equations are also plotted in Fig. 2. Using the temperature-dependent stress-strain curves, the thermal creep effect can be implicitly accounted for (Witteveen *et al.* 1977). Variations of the effective yield stress, $\sigma_{y\theta}$, the effective modulus of elasticity, E_{θ} , and the parameter, ζ_{θ} , with temperature levels are tabulated in Table 1. These variations of $\sigma_{y\theta}$ and E_{θ} are also illustrated in Fig. 3, where the initial yield stress, σ_{y20} , and the modulus of elasticity, E_{20} , are assumed respectively as 275 N/mm^2 and $205 \times 10^3 \text{ N/mm}^2$.

The coefficient of thermal expansion, α_{θ} , is often taken as $12 \times 10^{-6}/^{\circ}\text{C}$ when the temperature, θ , is between the room temperature of 20°C and below 200°C . For $200^{\circ}\text{C} < \theta \leq 600^{\circ}\text{C}$, α_{θ} is taken as $14 \times 10^{-6}/^{\circ}\text{C}$ (Lawson and Newman 1990). The coefficient of thermal expansion, α_{θ} , will be taken as $14 \times 10^{-6}/^{\circ}\text{C}$ for temperatures beyond 600°C . Besides, the coefficient of thermal expansion is considered to be independent of the types of steel, strength characteristics and temperature levels (Anderberg 1988).

4. Spring stiffness accounting for sectional plasticity

4.1. Determination of reduced plastic moment capacity

In the conventional second-order plastic hinge method, lumped plastic hinges are assumed to locate at the end nodes of an element for simulation of plasticity (see Fig. 4). The *section assemblage concept* (Chan and Chui 1997) is employed here for the derivation of non-linear spring stiffness for

Table 1 Mathematical approximations of yield stress and modulus of elasticity at elevated temperature

Temperature range	Yield stress $\sigma_{y\theta}$	Modulus of elasticity E_θ	Parameter ζ_θ
$80^\circ\text{C} < \theta \leq 200^\circ\text{C}$	$\sigma_{y20}(0.978 - 0.034\frac{\theta}{350})$	$E_{20}\left[1 - 2.8\left(\frac{\theta - 20}{1485}\right)^2\right]$	$\zeta_\theta = \frac{4600}{\theta} + \chi$
$200^\circ\text{C} < \theta \leq 400^\circ\text{C}$	Ditto	Ditto	$\zeta_\theta = \frac{2650}{\theta} + \chi$
$400^\circ\text{C} < \theta \leq 550^\circ\text{C}$	$\sigma_{y20}(1.553 - 0.155\frac{\theta}{100})$	Ditto	$\zeta_\theta = \frac{2400}{\theta} + \chi$
$550^\circ\text{C} < \theta \leq 600^\circ\text{C}$	$\sigma_{y20}(2.34 - 0.22\frac{\theta}{70})$	$E_{20}\left[1 - 3.0\left(\frac{\theta - 20}{1463}\right)^2\right]$	$\zeta_\theta = \frac{3900}{\theta} + \chi$
$600^\circ\text{C} < \theta \leq 690^\circ\text{C}$	$\sigma_{y20}(1.374 - 0.078\frac{\theta}{50})$	Ditto	$\zeta_\theta = \frac{3600}{\theta} + \chi$
$690^\circ\text{C} < \theta \leq 800^\circ\text{C}$	$\sigma_{y20}(1.120 - 0.128\frac{\theta}{100})$	Ditto	$\zeta_\theta = \frac{4600}{\theta} + \chi$

Remark : $\chi = \frac{\theta}{500 \log_e\left(\frac{\theta}{1750}\right)}$

sectional plasticity at element ends. The spring stiffness for bending about the major principal axis of I-sections has been formulated by Chan and Chui (1997). In this paper, bending about the minor

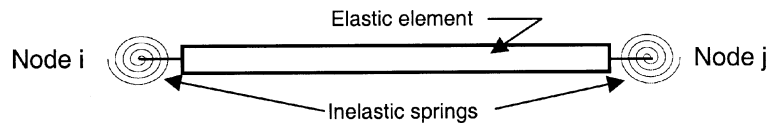


Fig. 4 A typical element used in the plastic hinge method

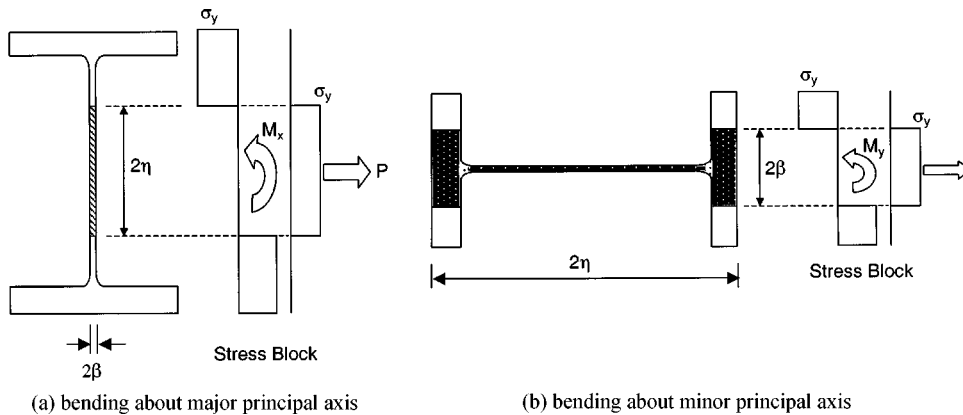


Fig. 5 Section assemblage concept in wide flange sections

principal axis is also given.

In the section assemblage concept, a given I-section is divided into three idealised rectangular strips illustrated in Fig. 5. These three strips represent the two flanges and the web. For annealed sections without the presence of residual stresses, the parameters η and β in Fig. 5, which define the yield region against resistance of the axial load, P , can be determined as follows:

Bending about major principal axis:

$$\eta = \frac{P}{2\sigma_y t_w} \quad \text{for } \eta \leq \frac{d}{2} \quad (3)$$

$$\eta = \frac{P - \sigma_y t_w d}{2B\sigma_{y\theta}} + \frac{d}{2} \quad \text{for } \frac{d}{2} < \eta \leq \frac{d}{2} + t_f \quad (4)$$

Bending about minor principal axis:

$$\eta = \frac{P}{2\sigma_y t_w} \quad \text{for } \eta \leq \frac{d}{2} \quad \text{and} \quad \beta = \frac{t_w}{2} \quad (5)$$

$$\eta = \frac{d}{2} \quad \& \quad \beta = \frac{1}{2} \left(\frac{P - dt_w \sigma_{y\theta}}{2t_f \sigma_{y\theta}} \right) \quad \text{for } \frac{d}{2} < \eta \leq \frac{d}{2} + t_f \quad \text{and} \quad 0 < \beta = \frac{B}{2} \quad (6)$$

in which t_f and t_w are respectively the thickness of the flange and the web; D is the overall depth of the I-section; d is the inner depth of the section; and B is the overall breadth (see Fig. 5). Once the parameters η and β are determined, the reduced plastic moment capacity, M_{pr} , can be simply computed as,

Bending about major principal axis:

$$M_{prx} = \sigma_y \left\{ B t_f (D - t_f) + t_w \left[\left(\frac{d}{2} \right)^2 - \eta^2 \right] \right\} \quad \text{for } \eta \leq \frac{d}{2} \quad \text{and} \quad \beta = \frac{t_w}{2} \quad (7)$$

$$M_{prx} = \sigma_{y\theta} B \left[\left(\frac{D}{2} \right)^2 - \eta^2 \right] \quad \text{for } \frac{d}{2} < \eta \leq \frac{d}{2} + t_f \quad \text{and} \quad \beta = \frac{t_w}{2} \quad (8)$$

Bending about minor principal axis:

$$M_{pry} = \sigma_{y\theta} \left\{ \frac{D t_f}{2} + \frac{t_w (\sigma_y t_w - P)}{4\sigma_{y\theta}} \right\} \quad \text{for } \eta \leq \frac{d}{2} \quad \text{and} \quad \beta = \frac{t_w}{2} \quad (9)$$

$$M_{pry} = \sigma_{y\theta} t_f \left(B - \frac{P - dt_w \sigma_{y\theta}}{2t_f \sigma_{y\theta}} \right) \left(B - \frac{P - dt_w \sigma_{y\theta}}{2} \right)$$

$$\text{for } \frac{d}{2} < \eta \leq \frac{d}{2} + t_f \quad \text{and} \quad 0 < \beta \leq \frac{B}{2} \quad (10)$$

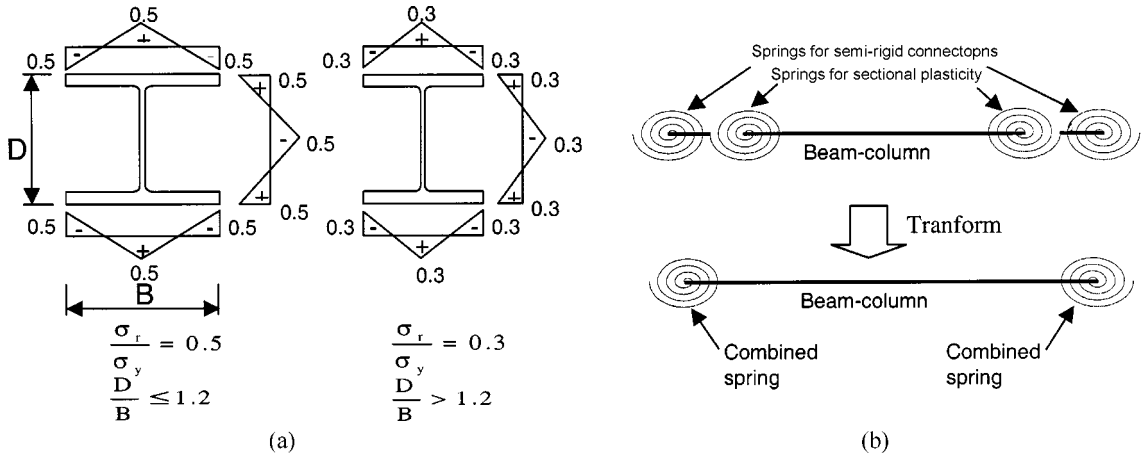


Fig. 6 Residual stress and spring models: (a) ECCSs (1983) residual stress pattern; (b) The combined spring-in-series model (Yau and Chan 1994)

4.2. Determination of sectional spring stiffness

Considering an end section of an element, the section spring stiffness, k_s , is assigned a large number relative to the element stiffness. In the present study, the value of $10^{10}E_\theta I/L$ is employed where I is the second moment of area and L is the element length. While the section is loaded beyond the initial yield surface, plastification will be initiated at its extreme outermost fibres. The initial or first-yield moment, M_{er} , suggested by Chan and Chui (1997) is,

$$M_{er} = (\sigma_{y\theta} - \sigma_{r\theta} - \sigma_a)Z \quad (11a)$$

where

$$\sigma_a = \frac{P}{A} \quad (11b)$$

in which $\sigma_{r\theta}$ is the residual stress at temperature, θ ; σ_a is the axial stress due to the axial force, P , A is the cross sectional area, and Z is the elastic section modulus. In Eq. (11), the residual stress, $\sigma_{r\theta}$, is assumed to be a function of temperature. When the section is at a high temperature, $\sigma_{r\theta}$ would be relieved and the material in the section will undergo a gradual relaxation according to the material law. The residual stress pattern may also change due to the thermal effect (Skinner 1976). The order of residual stress suggested by the European Convention for Construction Steelwork (ECCS 1983) shown in Fig. 6a is adopted. In this paper, the ratio of the residual stress, $\sigma_{r\theta}$, to the effective yield stress, $\sigma_{y\theta}$, at elevated temperature is considered to be constant.

Once yielding is initiated, the modified sectional spring stiffness can be calculated as

$$k_s = \frac{6\xi E_\theta I |M_{pr} - M|}{L |M - M_{er}|} \quad \text{for } M_{er} < M < M_{pr} \quad (12)$$

where M is the current bending moment at the section and ξ is an empirical parameter accounting for the temperature effect taken as,

$$\xi = \frac{1}{2E} \left(\frac{\sigma_{b\theta i}}{\varepsilon_{b\theta i}} + \frac{\sigma_{b\theta j}}{\varepsilon_{b\theta j}} \right) \quad \text{for bending about major principal axis} \quad (13)$$

$$\xi = \frac{1}{15} \quad \text{from curve-fitting for bending about major principal axis} \quad (14)$$

where $\sigma_{b\theta i}$ and $\sigma_{b\theta j}$ are respectively the bending stresses corresponding at nodes i and j under temperature, θ , $\varepsilon_{b\theta i}$ and $\varepsilon_{b\theta j}$ are their corresponding strains.

When the current moment, M , reaches the reduced plastic moment capacity determined from Section 4.1, the bending stiffness of the section will theoretically approach zero. However, the sectional spring stiffness, k_s , will be assigned as $10^{-10}E_\theta I/L$ in the present analysis for the sake of numerical stability.

5. Spring stiffness accounting for semi-rigid connections at elevated temperature

Although extensive investigations are available in literature, limited research was conducted on experimental and theoretical response of semi-rigid connections under fire. Among the available studies, El-Rimawi *et al.* (1997) and Leston-Jones *et al.* (1997) separately presented the moment-rotation curves for extended and flush end plate connections according to the available experimental results. These moment-rotation curves are expressed by the Ramberg-Osgood approximation (1943) in the form of,

$$\phi = \frac{M}{k_1} + 0.01 \left(\frac{M}{k_2} \right)^n \quad (15)$$

in which the curve-fitting parameters k_1 , k_2 and n are given by El-Rimawi *et al.* (1997) and Leston-Jones *et al.* (1997).

The stiffness of these connections can be simply obtained by taking the first derivative of Eq. (15) as,

$$k_c = \frac{dM}{d\phi} = \left[\frac{1}{k_1} + 0.01 \frac{n}{k_2} \left(\frac{M}{k_2} \right)^{n-1} \right]^{-1} \quad \text{for } |M| > 0 \quad (16)$$

For the case of $|M|=0$, the initial stiffness of these connections can then be obtained as,

$$k_c = \frac{dM}{d\phi} = k_1 \quad (17)$$

Eq. (17) is very useful for numerical simulation of semi-rigid connections in steel frames under fire. A numerical example to investigate the effect of these semi-rigid connections in a two-bay portal steel frame is evaluated in this paper.

6. Representation of combined effects of sectional plasticity and connection flexibility by spring-in-series model

The direct use of springs in series for representation of the effects of sectional plasticity and semi-rigid connections leads to computational complexity and significant truncating error may be resulted. Yau and Chan (1994) proposed the spring-in-series model in which the two springs can be

represented by a spring-in-series model in Fig. 6b. The stiffness of the resultant spring, k_{sc} , is expressed in terms of the stiffness for sectional plasticity, k_s , and semi-rigid connection, k_c , as

$$k_{sc} = \frac{k_s \cdot k_c}{k_s + k_c} \quad (18)$$

For rigid connections, the stiffness, k_c , is theoretically infinite and taken as $10^{10}E_\theta I/L$ in the present study.

7. Tangent stiffness matrix

The incremental moment versus rotation stiffness matrix of the proposed beam-column element can be written as,

$$\begin{Bmatrix} \Delta M_i \\ \Delta M_j \end{Bmatrix} = \begin{bmatrix} k_{11} & k_{12} \\ k_{21} & k_{22} \end{bmatrix} \begin{Bmatrix} \Delta \phi_i \\ \Delta \phi_j \end{Bmatrix} \quad (19a)$$

$$= \begin{bmatrix} \frac{4\xi E_\theta I}{L} + \frac{2PL}{15} & \frac{2\xi E_\theta I}{L} - \frac{PL}{30} \\ \frac{2\xi E_\theta I}{L} - \frac{PL}{30} & \frac{4\xi E_\theta I}{L} + \frac{2PL}{15} \end{bmatrix} \begin{Bmatrix} \Delta \phi_i \\ \Delta \phi_j \end{Bmatrix} \quad (19b)$$

and

$$\Delta P = \frac{E_\theta A}{L} \left[\Delta u_j - \Delta u_i + \frac{L}{30} (2\Delta \phi_i^2 - \Delta \phi_i \Delta \phi_j + 2\Delta \phi_j^2) \right] \quad (20)$$

in which ΔM is the incremental nodal moment; ΔP is the incremental axial force between two consecutive load levels; Δu is the incremental axial nodal displacement; and subscripts i and j represent respectively nodes i and j . As can be seen in Eqs. (19) and (20), the stiffness of the proposed beam-column element is dependent upon both E_θ and ξ_θ . However, using the spring-in-series model to account for the effects of sectional plasticity and connection flexibility described in the previous section, the tangent stiffness matrix, \underline{k}_T , for the proposed element can be expressed in terms of the modified stiffness coefficients \overline{k}_{11} , \overline{k}_{12} , \overline{k}_{21} and \overline{k}_{22} as follows (Yau and Chan 1994),

$$\begin{Bmatrix} \Delta M_i \\ \Delta M_j \end{Bmatrix} = \begin{bmatrix} \overline{k}_{11} & \overline{k}_{12} \\ \overline{k}_{21} & \overline{k}_{22} \end{bmatrix} \begin{Bmatrix} \Delta \phi_i \\ \Delta \phi_j \end{Bmatrix} \quad (21)$$

$$\overline{k}_{11} = k_{sci} - \frac{k_{sci}^2(k_{scj} + k_{22})}{\gamma} \quad (22)$$

$$\overline{k}_{12} = \frac{k_{sci}k_{scj}k_{12}}{\gamma} \quad (23)$$

$$\overline{k}_{21} = \frac{k_{sci}k_{scj}k_{21}}{\gamma} \quad (24)$$

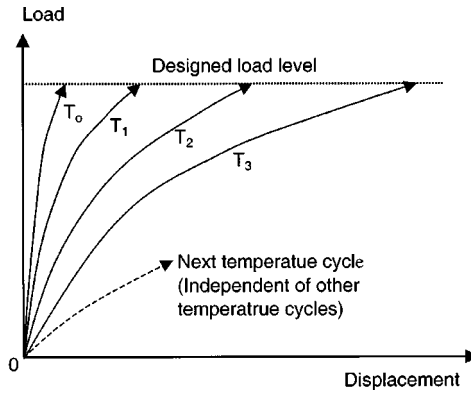


Fig. 7 Graphical illustration of the solution strategy of the present method

$$\bar{k}_{22} = k_{scj} - \frac{k_{scj}^2(k_{sci} + k_{11})}{\gamma} \quad (25)$$

in which

$$\gamma = (\bar{k}_{11} + k_{sci}) \cdot (\bar{k}_{22} + k_{scj}) - \bar{k}_{12}\bar{k}_{21} \quad (26)$$

and k_{11} , k_{12} , k_{21} and k_{22} have been given in Eq. (19).

8. Solution procedure

The present study employs the temperature rate-independent approach for the second order elastic-plastic analysis of steel frames under elevated temperature. Based on this approach, it is considered that the heating rate and history will not affect the structural behaviour of structures. Conventionally, some researchers applied the designed loads proportionally at the ambient condition. After reaching the desired loads, the temperature is then increased. The out-of-balance forces are determined at each increase of temperature level because of degradation of the mechanical properties of the material. In other words, the temperature is then increased until structural collapse. This procedure may lead to numerical divergence since the assigned load level may be higher than the load capacity of the frame.

The external load vector is applied from zero to its designed load magnitude using the Newton-Raphson increment/iterative procedure. By the present numerical procedure, the behaviour of a structural frame at a temperature can thus be considered as independent of the structural behaviour at other temperatures. On the basis of this assumption, a steel frame may be directly checked against any specified temperature for the required fire resistance period (see also Fig. 7).

In the proposed numerical procedure, thermal stress is taken into account using the Duhamel's analogy (Gatewood 1957, Ossenbruger 1973). The analogy is conducted in two steps. In the first step, the thermal forces are calculated on the assumption that each element is fully restrained at its ends against any axial and rotational movements. These thermal forces are subsequently added to the resistance of each element. To give the realistic values of these thermal forces in the second step, another vector of forces with equal and opposite magnitude is then superimposed to the vector

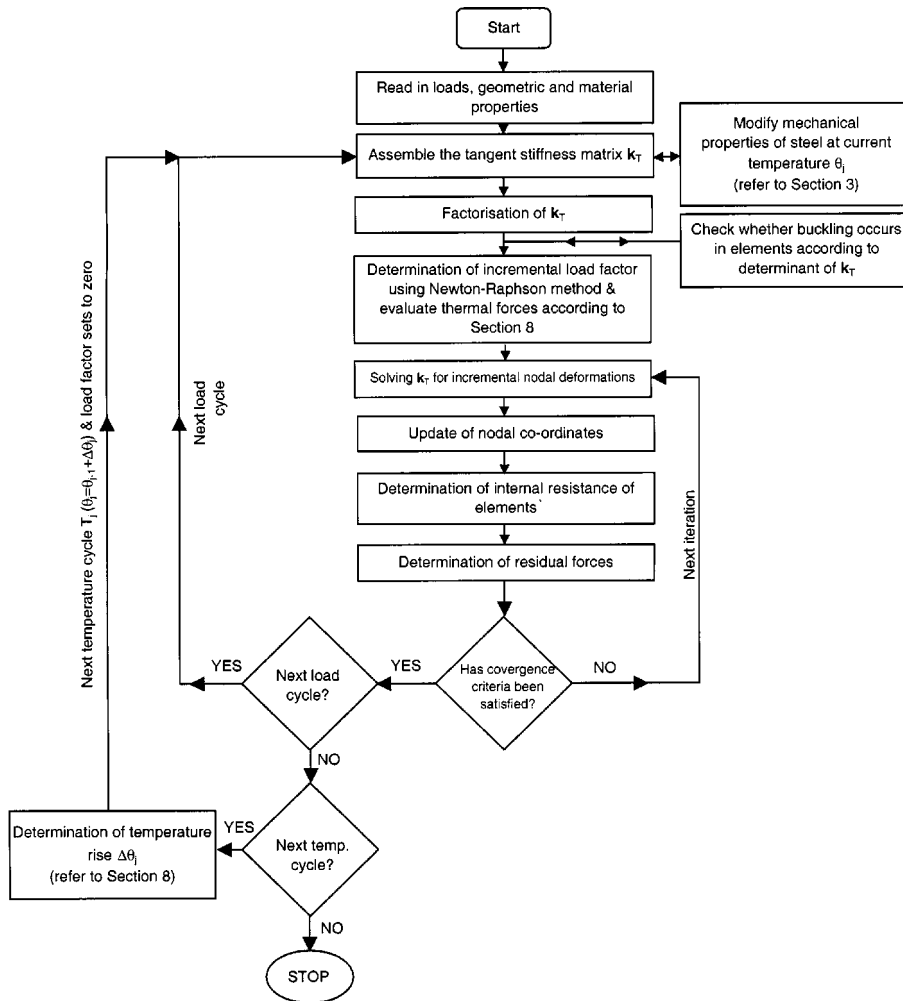


Fig. 8 Flowchart of the solution algorithm

of the external loads. It then forms the resultant vector of the applied forces. The Minimum Residual Displacement method (Chan 1988) is thus carried out for non-linear analysis in the step. Since uniform heating of steel elements is considered only, thermal axial forces is assumed in the present study. The temperature step is taken as 20°C.

The flowchart showing the overall solution strategy used for the present method is also illustrated in Fig. 8.

9. Numerical examples

For verification of the present method, the non-linear finite element program, GMNAF (1993), is modified to incorporate the temperature effect for steel frames. The experimental results of simply supported beams and frames reported by Rubert and Schaumann (1986) are compared with the present method. The

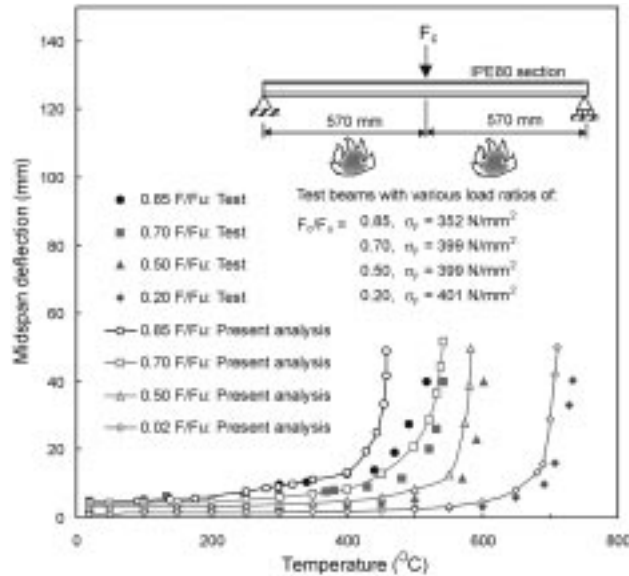


Fig. 9 Deflections at mid-span of a simply supported beams against temperature

numerical results of a beam-column by Franssen *et al.* (1994) are also selected for comparison. The fire test data of steel columns carried out in Bilbao (Azpiazu and Unanue 1993) are also used for verification. Finally, a two-bay portal frame with only one bay submitted to fire is analysed using various types of connections. In all analyses, the failure load is taken as the limit or elasto-plastic collapse load.

9.1. Experimental work by Rubert and Schaumann (1986)

9.1.1. Simply supported beams subjected to concentrated load at mid-span

Shown in Fig. 9 is the configuration of the four simply supported beams of IPE 80 I-section tested by Rubert and Schaumann (1986). This problem was later studied analytically by Kouhia *et al.* (1988) and others. In the tests, the beams were subjected to a constant load at mid-span and heated uniformly along the entire length. In this example, four beam-column elements are employed to model each beam. The structural behaviour of these beams under various load ratios of F_c/F_u ranging between 0.20 and 0.85, in which F_c and F_u are respectively the actual and ultimate concentrated loads, are evaluated. The modulus of elasticity is assumed as $210 \times 10^3 \text{ N/mm}^2$ and the actual yield stress of these beams loaded with different F_c/F_u values are shown in Fig. 9. In this figure, the variations of deflection at the mid-span for these beams against temperature are plotted and the test results reported by Rubert and Schaumann (1986) is also included in Fig. 9 for verification. It can be seen that the results predicted by the present method compares reasonably well with the tested results.

9.1.2. Small-scaled steel frames

The steel frames of reduced dimension of 1/6 to 1/4 to the original structure is shown in Fig. 10 and tested at elevated temperature by Rubert and Schaumann (1986). The experimental results of these frames were also adopted to verify the numerical results by other researchers, who included

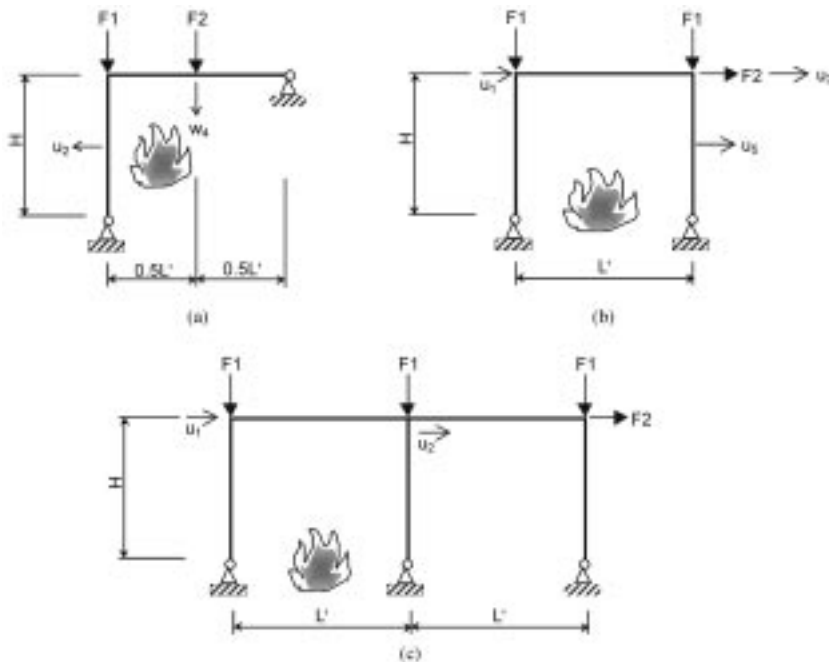


Fig. 10 The configurations of tests of frames of small scales: (a) EHR; (b) EGR; and (c) ZSR

Saab and Nethercot (1991) and Izzuddin *et al.* (2000). There are three series of geometry among these steel frames, which are the inverted L-shaped frames (EHR); the single-bay portal frames (EGR) and the double-bay portal frames (ZSR). These frames were composed of IPE80 I-sections with geometrical properties and measured yield strengths shown in Fig. 10. The modulus of elasticity at the ambient temperature is taken as $210 \times 10^3 \text{ N/mm}^2$. The frames were also adequately braced during the fire tests such that out-of-plane deflection was restricted. For the first two series (i.e., EHR and EGR), the frames were completely and uniformly heated and the critical temperatures were determined. The remarks for these fire tests are also depicted in the table. It should be noted that the beams in the frames EGR7/KR and EGR8/KR remained at room temperature during the fire tests. On the other hand, only the left bay of the portal frames ZSR is heated, whilst the right bay remains at ambient conditions. Furthermore, it was also concluded by Rubert and Schaumann (1986) that the measured column eccentricities and initial curvatures in these frames are insignificant and therefore ignored in present study.

In this example, the results are compared for cases using four and eight beam-column elements in modelling each steel member. The critical temperature predicted by the present method and the test results are reported in Table 2 and Fig. 11. It is found that all the predicted critical temperature is within ten percents of the test results, except for the frames EHR6, EGR5 and EGR6. The behaviour of the frames EHR3, EGR1 and ZSR1 in terms of displacements versus the temperature change is also plotted in Figs. 12, 13 and 14, with the numbers in brackets showing the total elements used in each model. As shown in these figures, the predicted curves are compared very well with the test results. In addition, the use of four or eight elements in modelling each steel member does not lead to significant difference in the predicted critical temperature for these frames.

Table 2 Test parameters and results of the frames tested by Rubert and Schaumann (1986)

System	L' (cm)	H (cm)	σ_{y20} (N/mm ²)	$F1$ (kN)	$F2$ (kN)	Critical temperature (°C)					Remark
						Test (C1)	Predicted (C2a)*	Diff. (C2a/C1)	Predicted (C2b)**	Diff. (C2b/C1)	
EHR1	119	117	395	56	14	600	626	1.0433	619	1.0317	Fully heated & bending about major axis
EHR2	124	117	395	84	21	530	559	1.0547	557	1.0509	do
EHR3	124	117	382	112	28	475	475	1.0000	478	1.0063	do
EHR4	125	150	389	20	5	562	529	0.9413	521	0.9270	Fully heated & bending about minor axis
EHR5	125	150	389	24	6	460	450	0.9783	433	0.9413	do
EHR6	125	150	389	27	6.7	523	374	0.7151	342	0.6539	do
EGR1b	122	117	382	65	2.5	533	476	0.8931	475	0.8912	Fully heated & bending about major axis
EGR1c	122	117	382	65	2.5	515	476	0.9243	475	0.9223	do
EGR2	122	117	385	40	1.6	612	580	0.9477	579	0.9461	do
EGR3	122	117	385	77	3	388	425	1.0954	423	1.0902	do
EGR4	122	117	412	77	3	424	435	1.0259	433	1.0212	do
EGR5	122	117	412	88	3.4	335	400	1.1940	397	1.1851	do
EGR6	122	117	412	88	3.4	350	400	1.1429	397	1.1343	do
EGR7/KR	122	117	320	68.5	2.6	454	466	1.0264	465	1.0242	do but cold beam
EGR8/KR	122	117	385	77	3	464	455	0.9806	454	0.9784	do but cold beam
ZSR1	120	118	355	74	2.85	547	504	0.9214	506	0.9250	Partly heated on left bay; bending about major axis
ZSR2	120	118	380	84.5	3.25	479	469	0.9791	467	0.9749	do
ZSR3	120	118	432	68.5	2.64	574	577	1.0052	576	1.0035	do

*Results predicted by the present method using eight elements per each beam and column.

**Results predicted by the present method using four elements per each beam and column.

9.2. Numerical results reported by Franssen *et al.* (1994)

9.2.1 Eccentrically loaded column

The column of HEB200 I-section shown in Fig. 15 is subject to uniform heating. It has been numerically studied by Franssen *et al.* (1994). The column is 4 m high with both pinned ends. Buckling is assumed to occur about the minor principal axis. The initial out-of-straightness is of a sinusoidal shape with the mid-height magnitude equal to 4 mm. The yield stress and modulus of elasticity at ambient temperature are respectively assumed as 235 N/mm² and 205×10³N/mm². The bi-triangular residual stress pattern suggested in ECCS (1983) is adopted with the maximum residual stress equal to 50% of the yield strength. The loading eccentricity is 100 mm from the centroid of the column, and it is considered that the eccentricity will amplify the effect due to the geometrical imperfection. The designed axial load is 250 kN with an eccentric moment of 25 kNm will be applied simultaneously to the frame.

Franssen *et al.* (1994) examined five different rigorous structural fire codes for the behaviour of this column. The variations of the results using these codes are found to be consistent and the

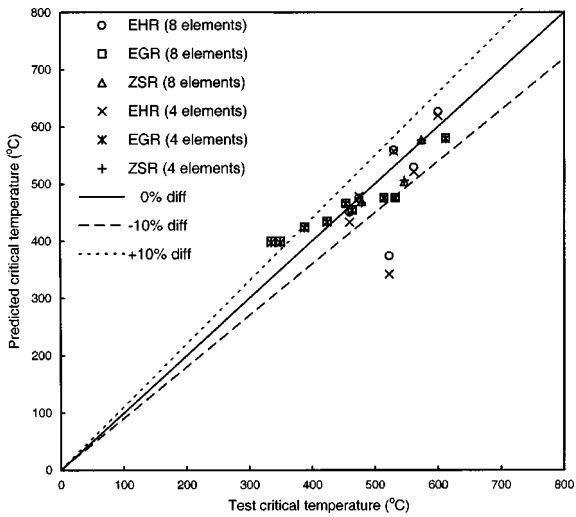


Fig. 11 Tested and predicted critical temperature for uniformly heated steel frames

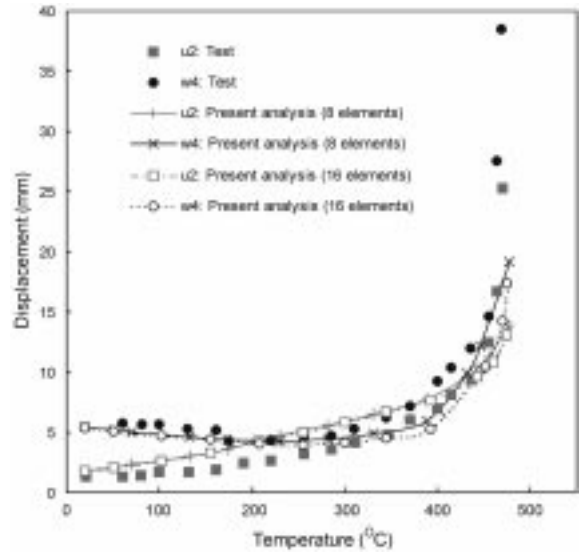


Fig. 12 Deformations of the frame EHR3 with temperature change

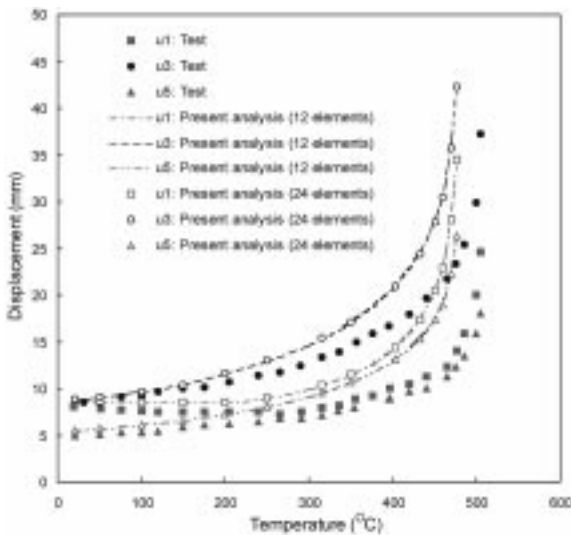


Fig. 13 Deformation of the frame EGR1 with temperature change

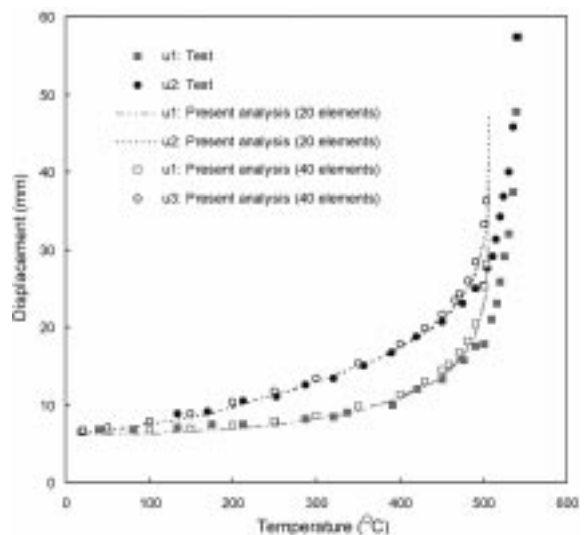


Fig. 14 Deformations of the frame ZSR1 with temperature change

difference is within 6%. In this example, the predicted result by the computer code SAFIR is reproduced for comparison against the present method. Eight elements are adopted by the proposed method to model this eccentrically loaded column.

The predicted horizontal displacement at mid-height is shown in Fig. 15, which shows a good agreement between the two curves. The critical temperature predicted by the present method is 441°C while the temperature by SAFIR is 432°C. The difference between these two methods is 2.1%.

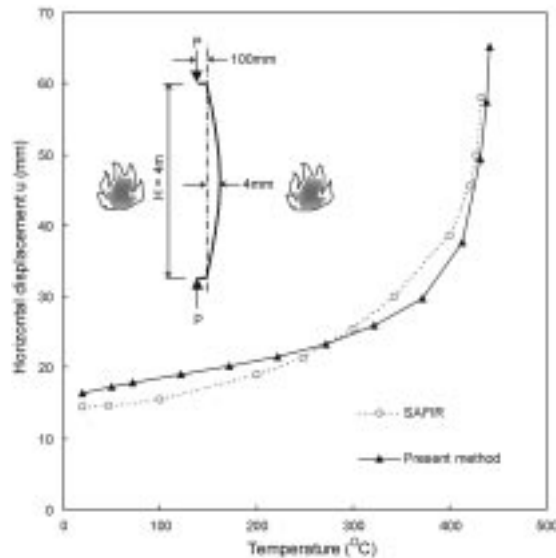


Fig. 15 Behaviour of the pinned-ended eccentrically loaded column

9.3. Fire tests of pinned-ended column from Bilbao

Fire tests on pinned-ended columns of HEA100 sections were conducted in the LABEIN laboratory in Bilbao and reported by Azpiazu and Unanue (1993). The eccentricity of loading was 5 mm in the tests and the experimental set-up was so arranged that buckling occurred only about the minor principal axis. The critical temperatures for the columns obtained from the tests were reproduced in Table 3. In the present study, each column is modelled by eight elements. The initial out-of-straightness of height/1000 at middle height and the residual stress suggested in ECCS (1983) are assumed. The modulus of elasticity at ambient temperature is taken as $205 \times 10^3 \text{ N/mm}^2$. The predictions by the present method are also included in Table 3 for comparisons. The accuracy of the present method in this example can be examined in Fig. 16. It is observed from the figure that the maximum difference between the tests and the present results for the critical temperature is about 10%.

9.4. Two-bay semi-rigid portal frame partially subjected to fire

The conventional practice in structural engineering assumes that beam-to-column connections are pinned in fire conditions since the actual behaviour of connection under fire is still not well understood. It is believed that this conventional approach leads to an over-conservative design. In this example, the influence of beam-to-column connections in the two-bay portal frame in Fig. 17 is examined at elevated temperature. The frame is made up of $305 \times 102 \times 33 \text{ UB}$ and only the bay on the left-hand side is under uniform heating, whilst the other bay remains at room condition. Pinned, rigid and semi-rigid connections at Points A and B in this figure are assumed and rigid connections are taken for the right-ended beam. For the semi-rigid connections, their temperatures are assumed equal to that of other steel members. Besides, the temperature-dependent curves for extended and flush end plate connections suggested by El-Rimawi *et al.* (1997) in Eq. (15) are

Table 3 Test and predicted results of pinned ended eccentrically loaded columns

No.	Section	σ_y (N/mm ²)	P (kN)	Length (mm)	Critical temperatures (°C)		
					Test (C1)	Present method (C2)	Ratio (C2/C1)
1	HEA100	290	361.5	513	532	531	0.9981
2	HEA100	298	110.0	513	694	717	1.0331
3	HEA100	290	292.5	1272	390	436	1.1179
4	HEA100	298	251.0	1271	474	529	1.1160
5	HEA100	281	174.2	2026	509	494	0.9705
6	HEA100	281	170.8	2020	485	502	1.0351
7	HEA100	281	172.9	2023	495	496	1.0020
8	HEA100	285	127.1	2770	457	488	1.0678
9	HEA100	290	72.7	2772	587	620	1.0562
10	HEA100	290	105.3	3510	446	447	1.0022
11	HEA100	298	90.4	3510	493	521	1.0568

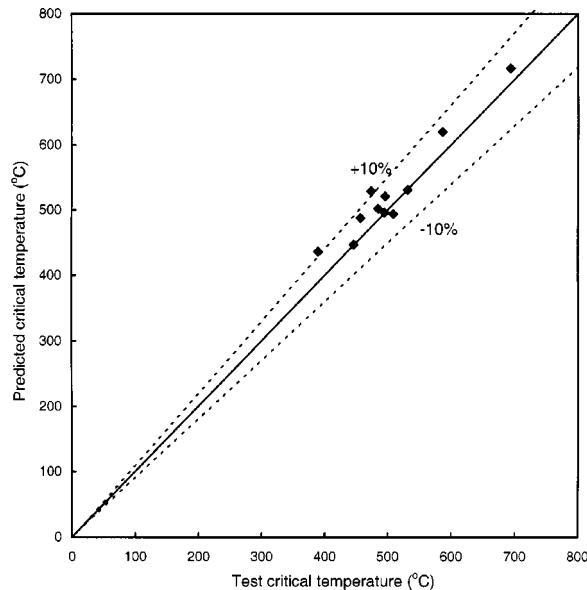


Fig. 16 Tested and predicted critical temperature for the pinned-ended columns bending about the minor principal axis

adopted. In consideration of the effects of beam size, El-Rimawi *et al.* (1997) suggested the following.

$$\phi = \frac{M}{\lambda^2 k_1} + 0.01 \left(\frac{M}{\lambda k_2} \right)^n$$

where

$$\lambda = \frac{D - 50}{303.8 - 50} \tag{28}$$

in which D is the overall depth of I-sections in millimeters and the parameter λ accounts for the actual beam size since the factors k_1 , k_2 and n given by El-Rimawi *et al.* (1997) are originally

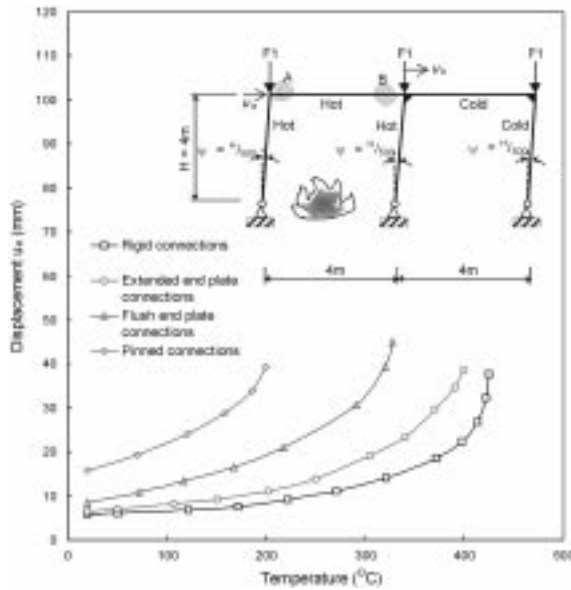


Fig. 17 Variations of displacement u_a with temperature increase

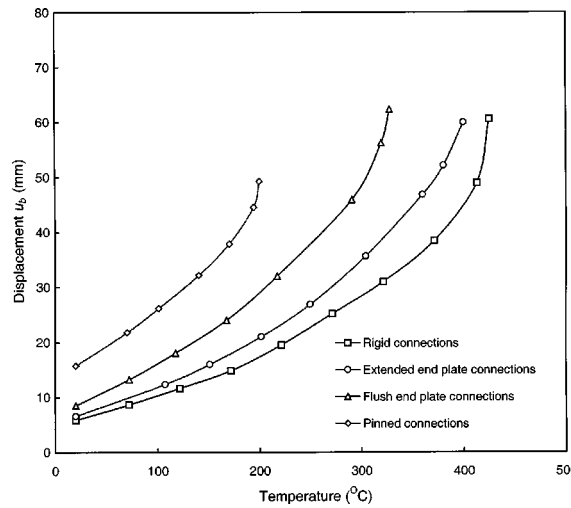


Fig. 18 Variations of displacement u_b with temperature increase

determined from the tests of 305×165×40UB section.

In this example, the modulus of elasticity and the yield strength for the steel sections are respectively $205 \times 10^3 \text{ N/mm}^2$ and 275 N/mm^2 . In the model, each of the beams and the columns is modelled by eight elements. The initial out-of-plumbness is considered to be 1/500 of its height. Every column is subjected to a load of 700 kN as shown in the same figure. The variations of horizontal displacements u_a and u_b are depicted in Figs. 17 and 18. It is observed that the assumption of pinned connections for fire design of steel frames will give an over-conservative and uneconomical design. Both figures reveal that the load-displacement curves

representing flush end plate connections is about between the curves for pinned and rigid connections. Moreover, the behaviour of the frame with extended end plate connections is also approximately the averaged performance for the rigid joints and the flush end plate connections.

From this example, consideration of stiffness of semi-rigid connections can provide much economical design for steel frames, when compared with the conventional assumption of pinned connections. Further extensive and detailed studies on the behaviour of different types of semi-rigid connections are required to improve the reliability of this type of advanced design.

10. Conclusions

The refined plastic hinge method has been practically used in the second-order elastic-plastic analysis of steel frames at ambient conditions. In the present study, the refined plastic hinge method is extended to study the behaviour of steel frames at elevated temperature on the basis of a 0.2% proof stress as the limiting stress. The time-independent approach is adopted and the efficient incremental/iterative solution strategy is employed for prediction of non-linear structural behaviour. From the numerical examples in this paper, the present method can provide efficient and accurate results for practical design. In contrast to other existing rigorous finite element programs that require heavy refinements throughout cross-sections and along element lengths, the present method is simple, efficient and provides a practical means for engineers to conduct fire analysis and design of steel frames. Based on the time-independent approach adopted, the sustainability of a given steel frame can be justified directly against any specified temperature level according to a particular fire resistance duration. Furthermore, the present method is a practical tool for the new performance-based design practice in fire safety engineering in evaluation of structural behaviour of rigid and semi-rigid steel structures.

Acknowledgements

Financial support from the Hong Kong Polytechnic University under grant G-V684 is gratefully acknowledged.

References

- Anderberg, Y. (1988), "Modelling steel behaviour", *Fire Safety J.*, **13**, 17-26.
- Azpiazu, W. and Unanue, J.A. (1993), Buckling curves of hot rolled H steel profiles submitted to fire", Report No. 97.798-2-ME/V, LABEIN, Bilbao, Spain.
- Bailey, C.G. (1998), "Development of computer software to simulate the structural behaviour of steel-framed buildings in fire", *Comp. & Structs.*, **67**, 421-438.
- Chan, S.L. (1988), "Geometric and material non-linear analysis of beam-columns and frames using the Minimum Residual Displacement Method", *Int. J. Num. Meth. Engng.*, **26**, 2657-2669.
- Chan, S.L. and Chui, P.P.T. (1997), "A generalized design-based elastoplastic analysis of steel frames by section assemblage concept", *Engineering Structures*, **19**(8), 628-636.
- ECCS (1983), "Ultimate limit state calculation of sway frames with rigid joints", Publication No. 33, European Convention for Constructional Steelwork, Brussels.

- El-Rimawi, J.A., Burgess, I.W. and Plank, R.J. (1997), "The influence of connection stiffness on the behaviour of steel beams in fire", *J. Constructional Steel Research*, **43**(1-3), 1-15.
- Eurocode 3 (1993), ENV 1993-1-1: Eurocode 3: Design of steel structures, Part 1.1: General rules, European Committee for Standardisation, Brussels.
- Franssen, J.M., Schleich, J.B., Talamona, D., Zhao, B., Twilt, L. and Both, K. (1994), "A comparison between five structural fire codes applied to steel elements", *Fire Safety Science-The Fourth International Symposium*, International Association for Fire Safety Science, 1125-1136.
- Furumura, F. and Shinohara, Y. (1978), "Inelastic behavior of protected steel beams and frames in fire", Report of the Res. Lab. of Engg. Mat., Tokyo, Japan.
- Gatewood, B.E. (1957), *Thermal Stress*, McGraw Hill Book Co., Inc., New York.
- GMNAF (1993), "Geometric and material non-linear analysis of frames - NAF series", *Users Reference Manual 9303-03*, The Hong Kong Polytechnic University, Hong Kong.
- Izzuddin, B.A., Song, L., Elnashai, A.S. and Dowling, P.J. (2000), "An integrated adaptive environment for fire and explosion analysis of steel frames - Part II: verification and application", *J. Constructional Steel Research*, **53**, 87-111.
- Kirby, B.R. and Preston, R.R. (1988), "High temperature properties of hot-rolled, structural steels for use in fire engineering design studies", *Fire Safety J.*, **13**, 27-37.
- Kouhia, R., Paavola, J. and Tuomala, M. (1988), "Modelling the fire behaviour of multistorey buildings", *I.A.B.S.E. 13th Congress Report*, Helsinki, 623-628.
- Lawson, R.M. (1987), "Fire engineering in the UK and Europe", *Steel Construction Today*, **1**, 159-165.
- Lawson, R.M. and Newman, G.M. (1990), "Fire resistant design of steel structures", *A Handbook to BS 5950: Part 8*, The Steel Construction Institute, UK.
- Leston-Jones, L.C., Burgess, I.W., Lennon, T. and Plank, R.J. (1997), "Elevated-temperature moment-rotation tests on steelwork connections", *Proc. Instn. Civ. Engrs. Structs. & Bldgs*, **122**, 410-419.
- Liew, J.Y.R., Tang, L.K., Holmaas, T. and Choo, Y.S. (1998), "Advanced analysis for the assessment of steel frames in fire", *J. Construct. Steel Res.*, **47**, 19-45.
- Ossenbruggen, P.J., Aggarwal, V. and Culver, C.G. (1973), "Steel column failure under thermal gradients", *J. Structural Division, ASCE*, **99**(ST4), 727-739.
- Poh, K.W. and Bennetts, I.D. (1995), "Behavior of steel columns at elevated temperatures", *J. Struct. Engg.*, ASCE, **121**(4), 676-684.
- Ramberg, W. and Osgood, W.R. (1943), "Description of stress-strain curves by three parameters", Technical Note No. 902, National Advisory Committee for Aeronautics.
- Rubert, A. and Schaumann, P. (1986), "Structural steel and plane frame assemblies under fire action", *Fire Safety Journal*, **10**, 173-184.
- Saab, H.A. and Nethercot, N.A. (1991), "Modelling steel frame behaviour under fire conditions", *Engg. Struct.*, **13**, 371-382.
- Song, L., Izzuddin, B.A., Elnashi, A.S. and Dowling, P.J. (2000), "An integrated adaptive environment for fire and explosion analysis of steel frames -Part I: Analytical models", *J. Construct. Steel Res.*, **53**, 63-85.
- Skinner, D.H. (1976), Discussion of "Effects of elevated temperature on structural members", *J. Structural Division, ASCE*, **102**(ST3), 685-687.
- Talamona, D., Franssen, J.M., Schleich, J.B. and Kruppa, J. (1997), "Stability of steel columns in case of fire: Numerical modeling", *J. Structural Engineering, ASCE*, **123**(6), 713-720.
- Wang, Y.C. and Moore, D.B. (1995), "Steel frames in fire: analysis", *Engg. Structs.*, **17**(6), 462-472.
- Witteveen, J., Twilt, L. and Bijlaard, F.S.K. (1977), "The stability of braced and unbraced frames at elevated temperatures, Stability of steel structures", Preliminary report, Liege.
- Yau, C.Y. and Chan, S.L. (1994), "Inelastic and stability analysis of flexible connected steel frames by spring-in-series model", *J. Structural Engineering, ASCE*, **120**(10), 2803-2819.